

^{13}C -Substituted sucrose: ^{13}C - ^1H and ^{13}C - ^{13}C spin coupling constants to assess furanose ring and glycosidic bond conformations in aqueous solution

Jennifer M. Duker and Anthony S. Serianni *

Department of Chemistry and Biochemistry, University of Notre Dame, Notre Dame, Indiana 46556 (USA)

(Received March 8th, 1993; accepted May 10th, 1993)

ABSTRACT

Sucrose (β -D-fructofuranosyl α -D-glucopyranoside, **1**), methyl α -D-fructofuranoside (**2**), and methyl β -D-fructofuranoside (**3**) have been prepared by chemical and/or enzymic methods with single sites of ^{13}C -substitution at C-1, C-2, C-3, and C-6 of the fructofuranosyl ring. ^1H (500 MHz) and ^{13}C (75 and 125 MHz) NMR spectra of **1**-**3** have been obtained, yielding ^1H - ^1H , ^{13}C - ^1H , and ^{13}C - ^{13}C spin coupling constants that were used to assess furanose ring and glycosidic bond conformations in aqueous ($^2\text{H}_2\text{O}$) solution. Results show that the conformational mobility of the furanosyl ring in **3** is altered when incorporated into **1**. Furthermore, ^{13}C - ^{13}C and ^{13}C - ^1H spin couplings across the glycosidic linkage suggest a ψ torsion angle different from that observed in the crystal (ϕ appears similar). Interplay between the strength of the exoanomeric effect and hydrogen bonding in solution may be responsible, in part, for the apparent conformational flexibility of **1**. In addition, spin couplings in **2** and **3** have been compared to those measured previously in α -D-threo-pentulofuranose (**4**) and β -D-threo-pentulofuranose (**5**), respectively, as a means to study the effect of glycosidation and hydroxymethyl substitution on the solution conformation of the 2-ketofuranose ring. The conversion of **4** to **2** is accompanied by minimal conformational change, whereas a significant change accompanies the conversion of **5** to **3**, showing that the effect of substitution on ring conformation depends highly on ring configuration before and after substitution.

INTRODUCTION

The structure and conformation of the disaccharide, sucrose (β -D-fructofuranosyl α -D-glucopyranoside, **1**) (Chart 1), have been the subjects of several previous investigations¹⁻⁷. Of particular interest has been the conformation of the glycosidic linkage in **1**, especially since data obtained in the crystalline¹ and solution²⁻⁷ states have led to uncertainty about whether linkage conformation is the same in both cases. At the heart of the problem is the potential role of

* Corresponding author.

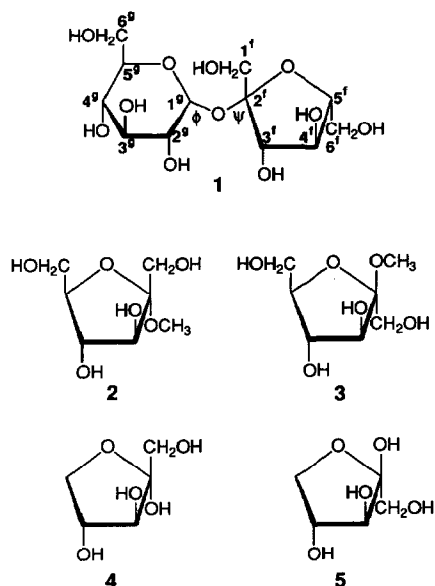


Chart 1.

hydrogen bonding, both intra- and inter-molecular (with solvent water), in affecting overall conformation in solution.

Mathlouthi and co-workers² concluded that the conformation of **1** in aqueous solution is concentration dependent; at low concentrations no intramolecular hydrogen bonds are present, whereas at higher concentrations, hydrogen bonding between OH-1^f ··· O-2^g and OH-6^f ··· O-5^g (throughout this paper, atoms of the *fructo* and *gluco* residues of **1** are denoted with “f” and “g” superscripts, respectively) occurs, as observed in the solid state. Davies and Christofides³ concluded from NMR data that two conformations of **1** exist in aqueous solution that differ in the location of a *single* hydrogen bond (OH-1^f ··· O-2^g and OH-3^f ··· O-2^g). Mulloy and co-workers⁴ measured several trans-glycoside ¹³C–¹H spin coupling constants in **1** and related oligosaccharides and concluded that the solid-state and solution conformations differ, whereas Bock and Lemieux⁵ applied HSEA calculations and concluded that **1** is conformationally rigid about the glycoside bond and that the solution and solid-state conformations are similar. The latter investigators also reported that the OH-1^f ··· O-2^g hydrogen bond found in the crystal structure is present in aqueous solution, while the second bond (OH-6^f ··· O-5^g) is not. McCain and Markley⁶ measured ¹³C spin–lattice relaxation times in **1** in solution and concluded that its conformation is similar to that observed in the crystalline state. Using NOE data, ¹³C–¹H spin-coupling constants and modeling calculations on **1** and its O-2^g-deoxy analogue, du Penhoat et al.^{7a} concluded recently that **1** does not exist as a single conformer in aqueous solution and that intramolecular hydrogen bonding is not an important determinant of

conformation. Adams and Lerner^{7b} have also concluded from studies of $^3J_{\text{HOCH}}$ values and hydroxyl proton exchange rates that there are no persistent hydrogen bonds in **1** in aqueous solution.

Tran and Brady⁸ have recently constructed an adiabatic potential energy surface for **1** that contains three low-energy conformational regions. Of these, two are similar in energy and contain the *S*-1/*S*-2 (region A) and the *S*-3/*S*-4 (region B) conformers*. Region A contains the global minimum energy conformer that is similar to the solid-state conformation and ~ 2.5 kcal/mol lower in energy than the *S*-3/*S*-4 conformers in region B. Given this small energy difference between conformers in the A and B regions, the degree of accuracy of these calculations and the potential effects of solvation not considered in these calculations, these results do not preclude the possibility that conformers in both regions A and B could be present in comparable amounts in aqueous solutions of **1**.

To probe further the solution behaviour of **1**, we have conducted a ^1H and ^{13}C NMR study of **1** and the model glycosides, methyl α - (**2**) and methyl β -D-fructofuranosides (**3**) (Chart 1). These compounds were prepared by chemical and/or enzymic methods with single sites of ^{13}C -substitution in the fructofuranosyl ring at C-1^f, C-2^f, C-3^f, and C-6^f. This labeling strategy allowed several ^{13}C - ^1H and ^{13}C - ^{13}C spin couplings within the 2-ketofuranosyl ring, and all of the available ^{13}C - ^1H and ^{13}C - ^{13}C couplings across the glycosidic bond, of **1** to be determined. We have compared these values, along with ^1H - ^1H spin couplings, in **1**–**3** to assess the effect of anomeric configuration and glycosidic bond formation on the conformational behavior of the fructofuranosyl ring. In addition, the NMR properties of **2** and **3** have been compared to those previously observed⁹ in the parent 2-ketofuranoses, α -D-*threo*-2-pentulofuranose (**4**) and β -D-*threo*-2-pentulofuranose (**5**) (Chart 1), in order to assess the effects of methyl glycosidation and hydroxymethyl substitution on 2-ketofuranosyl ring conformation.

EXPERIMENTAL SECTION

Materials.—D-Fructose, D-glucose, sucrose, uridine 5'-diphosphoglucose (UDPG, disodium salt), UDP-glucose: D-fructose 2-glycosyltransferase (sucrose synthetase, EC 2.4.1.13), and Dowex ion-exchange resins were purchased from Sigma Chemical Co. Immobilized D-xylose (D-glucose) isomerase (Takasweet Type Q, EC 5.3.1.5) was purchased from Miles Laboratories, Inc., and Bio-Gel P-2 gel permeation resin was purchased from Bio-Rad Laboratories. Deuterium oxide ($^2\text{H}_2\text{O}$, 98 atom% ^2H) and potassium (^{13}C)cyanide (K^{13}CN , 99 atom% ^{13}C) were obtained from Cambridge Isotope Laboratories. All other reagents were reagent grade and were used without further purification.

* See ref 8 for an explanation of *S*-1, *S*-2, etc.

D-(1-¹³C)Glucose^{10,11}, D-(2-¹³C)glucose^{11,12}, D-(3-¹³C)glucose¹¹, and D-(6-¹³C)glucose¹³ were prepared as previously described.

D-(¹³C)Fructose from D-(¹³C)glucose.—Immobilized D-xylose (D-glucose) isomerase was suspended in 0.5 M phosphate buffer (pH 7.4) in a 50-mL Erlenmeyer flask at 37°C for 0.5 h. D-(¹³C)Glucose (1.5 g, 8.3 mmol) was dissolved in the same buffer to give a final concentration of 1 M, and the solution was filtered (22- μ m filter) and added to the preincubated immobilized isomerase. The flask was sealed and agitated on a oscillating shaker at 37°C for 24 h. The immobilized enzyme was removed by filtration using a Whatman GF/B filter and washed with distilled water, and the filtrate and washings were combined and deionized by batchwise, separate treatment with excess Dowex SBR (OAc⁻) and Dowex HCR-W2 (H⁺) ion-exchange resins. After filtration to remove the resins, the deionized filtrate was concentrated at 30°C in vacuo to ~5 mL and applied to a column (4 \times 99 cm) containing Dowex 50 \times 8 (200–400 mesh) resin in the Ca²⁺ form¹⁴. The column was eluted with distilled water at a flow rate of ~1 mL/min, and the effluent was assayed with phenol–H₂SO₄ (ref 15). Two peaks eluted, with the first (elution volume, 595 mL) containing D-(¹³C)glucose and the second (elution volume, 840 mL) containing D-(¹³C) fructose. Fractions from each peak were pooled, and the two solutions were lyophilized to give dry white solids. Compounds were identified by their characteristic ¹³C chemical shifts¹⁶. Yields: D-(¹³C)glucose, 0.58 g, 3.2 mmol, 39%; D-(¹³C)fructose, 0.44 g, 2.4 mmol, 29%. Purity of the labeled fructose was > 98% determined by ¹³C NMR spectroscopy.

Methyl α - (2) and β -D-(¹³C)fructofuranosides (3) from D-(¹³C)fructose.—D-(¹³C)Fructose (0.46 g, 2.5 mmol) was dissolved in abs MeOH (30 mL) in a 100-mL round-bottom flask at room temperature. Concentrated H₂SO₄ (125 μ L) was added with stirring, and the flask was sealed with a stopper. Samples of the mixture were assayed by the ferricyanide test¹⁷ to monitor the disappearance of reducing sugar (~70 min). The reaction was interrupted by passing the solution through a 3 \times 41 cm column containing Amberlite IRA-68 in the OH⁻ form (packed and prewashed with abs MeOH), using abs MeOH as the eluent. When all of the sugar had eluted, as determined by phenol–H₂SO₄ (ref 15), the effluent was concentrated to a syrup at 30°C in vacuo, and the resulting syrup was dissolved in CO₂-free distilled water and applied to a column (2.5 \times 105 cm) containing Dowex 1 \times 8 (200–400 mesh) ion-exchange resin in the OH⁻ form¹⁸. The column was eluted with CO₂-free distilled water at a flow rate of ~1 mL/min, and fractions (14.5 mL) were collected and assayed with phenol–H₂SO₄ (ref 15). Three peaks were detected with elution volumes of 540, 1247, and 2538 mL. Peak fractions were pooled and concentrated at 30°C in vacuo to give clear, colorless syrups. The furanosides were identified by their characteristic ¹³C chemical shifts¹⁶: methyl β -D-fructopyranoside (peak 1), methyl β -D-fructofuranoside 3 (peak 2), and methyl α -D-fructofuranoside 2 (peak 3). Yield: 2, 0.22 g, 1.1 mmol, 44%; 3, 0.23 g, 1.2 mmol, 48%. Purity of 2 and 3 was > 98% determined by ¹³C and ¹H NMR spectroscopy (Figs. 1 and 2).

β -D-(^{13}C)Fructofuranosyl- α -D-glucopyranoside [sucrose (1)] from D-(^{13}C)fructose.—UDPG (0.66 g, 1.1 mmol) and D-(^{13}C)fructose (0.18 g, 1.0 mmol) were added to a conical tube containing 5.0 mL of deionized water, 100 mL of M MgCl_2 , and a small stirring bar. The tube was purged with N_2 and sealed immediately with a rubber septum adapted to securely hold a pH microelectrode (Microelectrodes, Inc.). The solution pH was adjusted with M KOH to pH 8.2, and this pH was maintained throughout the course of the reaction. Sucrose synthetase (EC 2.4.1.13) (25 units) was added with a syringe, the solution was mixed for a brief period, and the resulting solution was incubated at 37°C under N_2 . After 5 h, a 1.0 mL sample was withdrawn for analysis by TLC and/or NMR spectral analysis. This sample was heated to 100°C for 10 min to terminate the reaction and analyzed by TLC (silica gel) using 5:3:2 butanol–EtOH–water as the solvent. TLC plates were sprayed with 2 N H_2SO_4 followed by heating (hot plate) to visualize spots. Fructose migrated slightly faster than sucrose. Alternatively, when ^{13}C -substituted fructoses were used, a ^{13}C NMR spectrum was obtained to determine the extent of the reaction since the signals from the labeled fructose and sucrose could be readily detected and distinguished. After 5 h, an additional 25 units of enzyme were added, and the reaction was allowed to continue for an additional 5 h, at the end of which time the reaction was essentially complete as determined by TLC.

The mixture was applied to a column (1.5 \times 20 cm) containing Dowex SBR (OAc^-) ion-exchange resin, and the column was eluted with deionized water until all of the sugar had eluted, as assayed by phenol– H_2SO_4 (ref 15). The effluent was adjusted to pH 5.0 by batchwise treatment with Dowex HCR-W2 (H^+) ion-exchange resin; pH < 5.0 was avoided to prevent the hydrolysis of 1. After removal of the resin by filtration, the filtrate was concentrated at 30°C in vacuo to a syrup, the syrup was dissolved in a minimum quantity of distilled water, and the solution was applied to a column (4 \times 99 cm) containing Dowex 50 \times 8 (200–400 mesh) ion-exchange resin in the Ca^{2+} form¹⁴. The column was eluted with distilled water at a flow rate of \sim 1 mL/min and fractions (14 mL) were collected and assayed with phenol– H_2SO_4 (ref 15). Fractions defining two peaks with elution volumes of 480 and 870 mL were pooled and concentrated at 30°C in vacuo to syrups. D-(^{13}C)Fructose (peak 1) and (^{13}C)sucrose (peak 2) were identified by their characteristic ^{13}C chemical shifts¹⁶.

The sucrose fraction contained residual salts that were subsequently removed by two methods. In method 1, the sucrose syrup was dissolved in a minimum volume of distilled water and the solution was applied to a column (2.5 \times 40 cm) containing Bio-Gel P-2 resin. Elution of the column with distilled water gave one peak containing (^{13}C)sucrose that was free of contaminating salts. Method 2 afforded a better yield by passing the sucrose solution through a column (1.5 \times 20 cm) containing Dowex SBR (OAc^-) ion-exchange resin and carefully treating the effluent batchwise with Dowex HCR-W2 (H^+). After removal of the resin by filtration, the solution was concentrated to a syrup at 30°C in vacuo. Evaporation

from distilled water was repeated twice more to remove residual acetic acid. The product **1** was characterized by ^1H and ^{13}C NMR using authentic unlabeled sucrose as the standard. Isolated yields of **1** were $\sim 25\%$ (Bio-Gel P2 purification) and $\sim 60\%$ (Dowex SBR purification) based on D-fructose.

NMR spectroscopy.—High-resolution ^1H -decoupled ^{13}C (125 MHz) and ^1H (500 MHz) NMR spectra were obtained on a Varian VXR-500S, 500-MHz FT-NMR spectrometer operating at 25°C in the quadrature-phase mode. High-resolution ^1H -decoupled ^{13}C NMR spectra (75 MHz) were obtained on a General Electric GN-300, 300-MHz FT-NMR spectrometer operating at 25°C . FIDs were zero-filled at least once and processed with resolution enhancement in cases where high digital resolution and maximal resolution were desired for the measurement of small couplings. ^1H -Decoupled ^{13}C INADEQUATE NMR spectra¹⁹ were acquired on the GN-300 FT-NMR spectrometer as previously described^{20,21}. Coupling signs were not determined for J_{CC} and J_{CH} , and thus only their absolute values are reported. Coupling constants reported as “nc” (no coupling) implies a $J < \sim 8$ Hz for J_{CC} and $< \sim 0.5$ Hz for J_{HH} and J_{CH} .

Computer simulation of 500 MHz ^1H NMR spectra was performed using the LAOCN5 program as implemented in the FTNMR program (VAX version) available from Hare Research, Inc. of Woodinville, WA²². The computations were conducted on a Digital VaxStation 3200 minicomputer equipped with a Tektronix CX4107 graphics terminal.

RESULTS

Synthesis of ^{13}C -substituted fructofuranosides and sucrose.—Enzyme-catalyzed glucose–fructose interconversion by immobilized D-xylose (D-glucose) isomerase (EC 5.3.1.5) was used to prepare ^{13}C -substituted D-fructose, from which were prepared **1–3**. The reaction conditions gave a low yield ($\sim 30\%$) of fructose, but the residual unreacted labeled glucose was recovered. Methyl glycosidation of D-fructose to give **2** and **3** was performed at room temperature to maximize the formation of the kinetically favored furanosides²³, which were produced in $\sim 90\%$ yield.

The enzymic synthesis of (^{13}C)sucrose **1** from (^{13}C)fructose and UDP-glucose using sucrose synthetase (EC 2.4.1.13) gave different overall yields depending on the method of purification. Chromatography on Bio-Gel P-2 gave a poorer yield ($\sim 25\%$) compared to purification with ion-exchange resins ($\sim 60\%$). The reduced yield of the former procedure is probably caused by binding of sucrose to the gel under the conditions used for elution.

^{13}C and ^1H NMR spectra of natural and ^{13}C -substituted methyl α - (2**) and β -D-fructofuranosides (**3**).**—The ^{13}C chemical shifts of the C-2 anomeric carbons were used to identify the anomeric glycosides, **2** and **3**. These assignments (Table I) were made in part by analogy to those for the parent 2-ketopentofuranoses, D-erythro-pentulofuranose and D-threo-pentulofuranose, in which the more shielded

TABLE I

 ^{13}C NMR chemical shifts of methyl D-fructofuranosides **2** and **3** in $^2\text{H}_2\text{O}$

Compound	Chemical shift (ppm) ^a						
	C-1	C-2	C-3	C-4	C-5	C-6	OCH ₃
2	58.6	109.0	80.8	78.1	84.0	62.0	49.0
3	61.6	105.6	78.7	76.9	83.1	64.5	50.8

^a Values are reported relative to the anomeric carbon of α -D-(1- ^{13}C)mannopyranose (95.5 ppm) and are accurate to ± 0.1 ppm.

anomeric C-2 carbon was assigned to that anomer having O-2 and O-3 *cis*⁹. Thus, the C-2 signal of **3** is found upfield from that of **2** (Table I). These assignments were confirmed by $^3J_{\text{C-1,H-3}}$, which may be used to assign anomeric configuration in 2-ketofuranosyl rings^{9,24}. This coupling assumes a value of ~ 2.3 Hz when C-1 and H-3 are *cis*, and a value of ≤ 0.3 Hz when these atoms are *trans*. In **2**, $^3J_{\text{C-1,H-3}} = 0$ Hz, whereas $^3J_{\text{C-1,H-3}} = 2.1$ Hz in **3** (Table II). Likewise, in **1**, $^3J_{\text{C-1f,H-3f}} = 1.7$ Hz, as expected for the β -configuration in the disaccharide. The remaining ^{13}C signal assignments for **2** and **3** (Table I) were made with the assistance of selective ^{13}C -substitution (at C-1, C-2, C-3, and C-6) by either observing the enhanced labeled carbon signal or the large (42–53 Hz) one-bond ^{13}C – ^{13}C spin-coupling contained in signals of carbons adjacent to the labeled site (Table III, Fig. 1).

TABLE II

 ^{13}C – ^1H spin-coupling constants^a in methyl D-fructofuranosides **2** and **3** in $^2\text{H}_2\text{O}$

Coupled nuclei	Compound	
	2	3
C-1, H-1	143.4	~ 144.1
C-1, H-1'	145.6	~ 143.8
C-1, H-3	nc	2.1
C-2, H-1	4.3	4.2
C-2, H-1'	2.2	2.3
C-2, H-3	~ 2.7	br
C-2, H-4	1.7	nc
C-2, H-5	nc	2.8
C-2, OCH ₃	3.7	3.6
C-3, H-1	2.9	3.3
C-3, H-1'	br	2.4
C-3, H-3	obsc	145.9
C-3, H-4	obsc	5.7
C-3, H-5	obsc	nc
C-6, H-4	obsc	5.3
C-6, H-5	obsc	br
C-6, H-6		~ 141.8
C-6, H-6'		143.4

^a Values are reported in Hz and are accurate to ± 0.1 Hz. 'Obsc' denotes obscured signals, 'nc' denotes no coupling, and 'br' denotes broadened signals. No entry means that the coupling was not measured.

TABLE III

 ^{13}C – ^{13}C spin-coupling constants ^a in methyl D-fructofuranosides **2** and **3** in $^2\text{H}_2\text{O}$

Coupled nuclei	Compound	
	2	3
C-1, OCH ₃	1.8	2.3
C-1, C-2	53.0	52.4
C-1, C-3	nc	2.2
C-1, C-4	nc	nc
C-1, C-5	2.7	1.9
C-2, OCH ₃	2.3	2.4
C-2, C-3	48.4	46.7
C-2, C-4	3.0	3.9
C-2, C-5	nc	nc
C-2, C-6	2.3	nc
C-3, OCH ₃	2.4	1.8
C-3, C-4	40.8	41.1
C-3, C-5	2.8	4.6
C-3, C-6	2.0	2.5
C-6, C-4	1.5	2.0
C-6, C-5	42.5	42.3

^a Values are reported in Hz and are accurate to ± 0.25 Hz. The entry 'nc' denotes no coupling.

These assignments are consistent with those reported previously by Angyal and Bethell²⁵.

Several longer-range ^{13}C – ^{13}C spin-couplings (e.g., $^2J_{\text{CC}}$, $^3J_{\text{CC}}$) were obtained from the inspection of ^{13}C NMR spectra of ^{13}C -labeled **2** and **3** (Table III). For example, the 75 MHz ^1H -decoupled ^{13}C NMR spectrum of (3- ^{13}C)**3** (Fig. 1) gave doublets for each unlabeled carbon signal, indicating the presence of ^{13}C – ^{13}C spin-coupling between C-3 and each carbon in the molecule (Table III).

The 500 MHz ^1H NMR spectrum of **3** is essentially first order, whereas that of **2** is non-first order. Thus, the ^1H chemical shifts and ^1H – ^1H couplings of **3** were obtained directly from the spectrum (Tables IV and V) using the characteristic H-3 doublet of the 2-ketofuranose ring (H-3 is coupled only to H-4) to initiate the assignment process. In contrast, the corresponding parameters for **2** were obtained via spectral simulation by computer. ^{13}C – ^1H spin-couplings in ^{13}C -substituted **2** and **3** were determined (Table II) from the ^1H NMR spectra by observing the added splitting in the signals of protons coupled to the labeled carbon (Fig. 2). All available ^{13}C – ^1H couplings to the labeled carbons were obtained for **3**, whereas for **2** several couplings could not be measured due to resonance overlap.

^{13}C and ^1H NMR spectra of natural and ^{13}C -substituted sucrose (**2**). Sucrose (**1**) was prepared with site-specific ^{13}C -substitution at C-1^f, C-2^f, C-3^f, and C-6^f, and the labeled derivatives were used to make carbon signal assignments in the *fructo* residue (Table VI) as described above for ^{13}C -substituted **2** and **3**. These assignments were consistent with those previously reported^{5,26}. 1D ^{13}C INADEQUATE

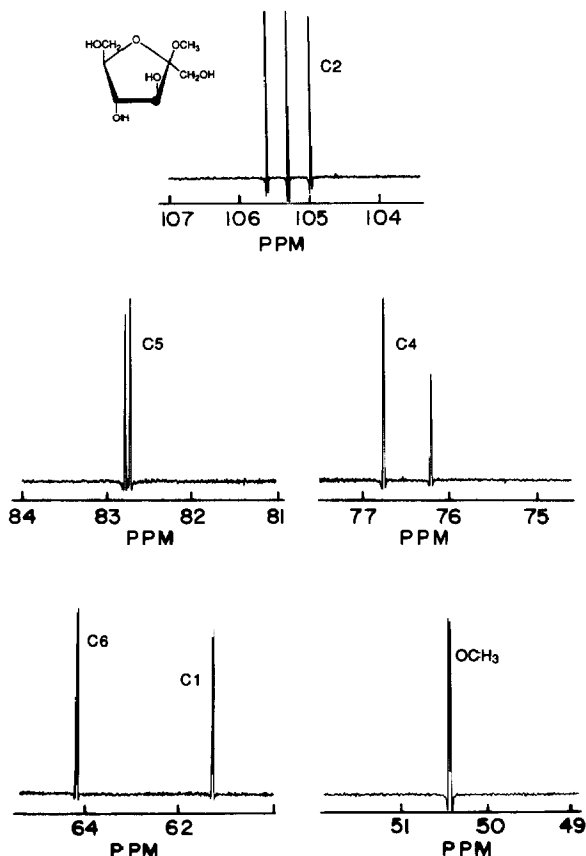


Fig. 1. Expanded natural abundance regions of the resolution-enhanced ^1H -decoupled ^{13}C NMR spectrum (75 MHz) of **3** labeled with ^{13}C (99 atom%) at C-3. All carbon signals are split, indicating the presence of ^{13}C - ^{13}C spin coupling: C-1, 2.2 Hz; C-2, 46.7 Hz; C-4, 41.1 Hz; C-5, 4.6 Hz; C-6, 2.5 Hz (see Table III). The triplet pattern observed for C-2 is caused by the presence of ($2\text{-}^{13}\text{C}$)**3** as a minor impurity ($\sim 1\%$) in the sample.

spectra of (^{13}C)-labeled **1** were collected with different mixing times in order to selectively observe carbons coupled to the labeled site^{20,21} (Table VII). For example, INADEQUATE spectra of ($2\text{-}^{13}\text{C}$)**1** (Fig. 3) show the selective detection

TABLE IV

^1H NMR chemical shifts in methyl D-fructofuranosides **2** and **3** in $^2\text{H}_2\text{O}$

Compound	Chemical shift (ppm) ^a							
	H-1	H-1'	H-3	H-4	H-5	H-6	H-6'	OCH ₃
2	3.87	3.75	4.18	4.04	4.05	3.90	3.78	3.41
3	3.80	3.73	4.25	4.13	3.94	3.88	3.73	3.41

^a Values are reported relative to internal HO²H (4.80 ppm) and are accurate to ± 0.01 ppm.

TABLE V

 ^1H - ^1H spin-coupling constants a in methyl D-fructofuranosides **2** and **3** in $^2\text{H}_2\text{O}$

Coupled nuclei	Compound	
	2	3
H-1, H-1'	-12.4	-12.3
H-3, H-4	3.2	8.2
H-4, H-5	6.0	~7.5
H-5, H-6	3.1	3.2
H-5, H-6'	5.6	7.1
H-6, H-6'	-12.3	-12.3

 a Values are reported in Hz and are accurate to ± 0.1 Hz.

of C-3^f and C-1^f (via $^1J_{\text{CC}}$) at short mixing times, and the detection of C-1^g, C-5^f, C-4^f, and C-2^g at longer mixing times (via $^2J_{\text{CC}}$ or $^3J_{\text{CC}}$). This method suppresses the detection of carbons not spin-coupled to the labeled site, thereby simplifying spectra without sacrificing information content.

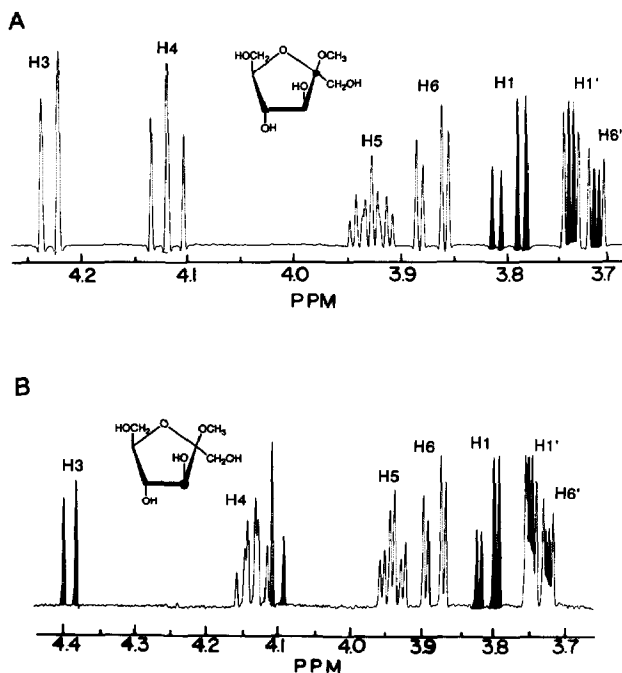


Fig. 2. Partial ^1H NMR spectra (500 MHz, resolution enhanced) of **3** singly labeled with ^{13}C (99 atom%) at C-2 (A) and C-3 (B), showing signal assignments. Filled signals in A and B are due to H-1 and H-1'; hatched signals in B are due to H-3, which is split by $^1J_{\text{C-3,H-3}}$. Longer-range ^{13}C - ^1H couplings were determined by comparing multiplets observed in the enriched spectra to those observed in the spectrum of the natural (unlabeled) compound.

TABLE VI

 ^{13}C NMR chemical shifts of β -D-fructofuranosyl α -D-glucopyranoside (sucrose, **1**) in $^2\text{H}_2\text{O}$

Residue	Chemical shift (ppm) ^a											
	C-1 ^f	C-2 ^f	C-3 ^f	C-4 ^f	C-5 ^f	C-6 ^f	C-1 ^g	C-2 ^g	C-3 ^g	C-4 ^g	C-5 ^g	C-6 ^g
β -D-Fructofuranosyl	63.6	106.0	78.7	76.3	83.7	64.7						
α -D-Glucopyranosyl							94.5	73.4	74.9	71.5	74.7	62.4

^a Values are reported relative to the anomeric carbon of α -D-(1- ^{13}C)mannopyranose (95.5 ppm) and are accurate to ± 0.1 ppm.

The ^1H NMR spectrum of **1** has been previously interpreted^{5,26}. At 500 MHz, the signals of H-1^g, H-2^g, H-3^g, H-4^g, H-3^f, H-4^f, and H-5^f are cleanly resolved, whereas those of the remaining protons overlap in a small region (3.88–3.93 ppm) (Table VIII). Thus, in this study, only those ^1H – ^1H couplings involving the former group of protons were evaluated (Table IX). Likewise, potential ^{13}C – ^1H coupling was assessed only in the well-resolved proton signals of ^{13}C -substituted **1** (Table X).

The choice of sites for ^{13}C -substitution (C-1^f, C-2^f, C-3^f, and C-6^f) was made to maximize ^{13}C – ^{13}C and ^{13}C – ^1H coupling data pertinent to fructofuranosyl ring and glycosidic bond conformation of **1**. With respect to the latter, all possible *trans*-glycoside ^{13}C – ^{13}C and ^{13}C – ^1H spin couplings were evaluated (Fig. 4).

Analysis of spin–spin coupling constants in methyl α - and β -D-fructofuranosides (2 and 3) and sucrose (1).—A. *One-bond ^{13}C – ^{13}C spin-couplings.* The magnitudes

TABLE VII

 ^{13}C – ^{13}C spin-coupling constants^a in β -fructofuranosyl α -D-glucopyranoside (sucrose, **1**) in $^2\text{H}_2\text{O}$

Coupled nuclei	Sucrose 1
C-1, C-2	52.6
C-1, C-3	2.1
C-1, C-4	nc
C-1, C-5	nc
C-1, C-1 ^g	nc
C-2, C-3	46.1
C-2, C-4	4.1
C-2, C-5	br
C-2, C-6	nc
C-2, C-1 ^g	2.4
C-2, C-2 ^g	2.0
C-3, C-4	39.4
C-3, C-5	4.9
C-3, C-6	~ 2.5
C-3, C-1 ^g	nc
C-6, C-4	nc
C-6, C-5	42.5

^a Values are reported in Hz and are accurate to ± 0.25 Hz. The entry 'nc' denotes no coupling. Carbons within the glucopyranosyl residue are denoted by a 'g' superscript; all other carbons are within the fructofuranosyl residue. br, Broadened resonance.

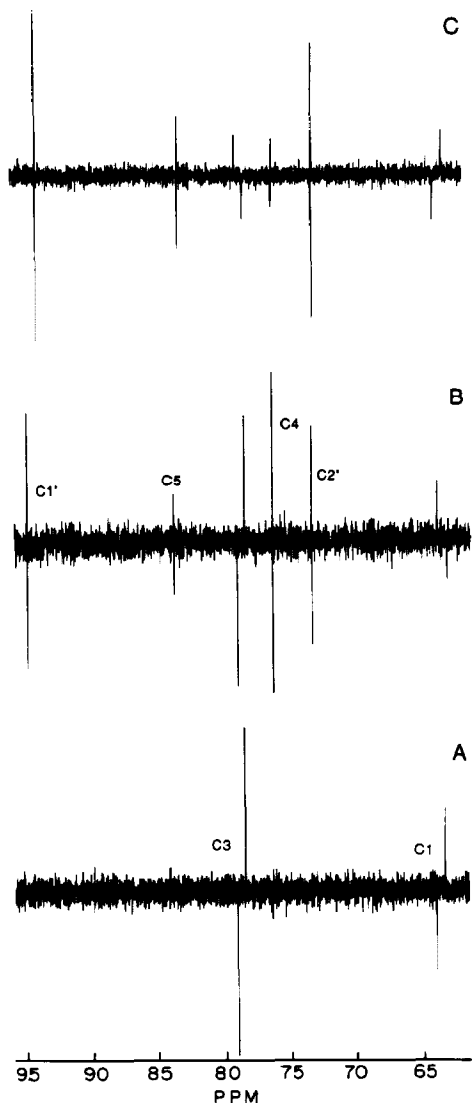


Fig. 3. INADEQUATE ^{13}C NMR spectra (75 MHz) obtained on $(2^f\text{-}^{13}\text{C})\mathbf{1}$, showing the effect of different mixing times on signal detection. Only the natural abundance region is shown. Mixing times of 6.0 ms (A), 50 ms (B) and 100 ms (C) were used, generating edited spectra containing signals of directly-bonded (to the labeled site) carbons (e.g., C-1^f and C-3^f) at shorter times (A), and signals of carbons more distant from the labeled site (e.g., C-4^f , C-5^f , C-1^s , C-2^s) at longer times (C). Only those carbons that couple to the labeled site are detected.

of one-bond ^{13}C – ^{13}C spin-couplings in the β -D-fructofuranosyl rings of 1–3 (Tables III and VII) depend on the number of oxygen substituents appended to the coupled carbons and on whether the C–C bond is exocyclic or endocyclic. In general, $^1J_{\text{CC}}$ increases with the number of oxygen substituents on the C–C

TABLE VIII
¹H NMR chemical shifts of β-D-fructofuranosyl β-D-glucopyranoside (sucrose, 1) in ²H₂O

Residue	Chemical shift (ppm) ^a										
	H-1 ^g	H-2 ^g	H-3 ^g	H-4 ^g	H-5 ^g	H-6/H-6' ^g	H-1/H-1' ^f	H-3 ^f	H-4 ^f	H-5 ^f	H-6/H-6' ^f
α-D-Glucopyranosyl	5.49	3.63	3.83	3.54	3.88–3.93	3.88–3.93	3.75	4.29	4.12	3.96	3.88–3.93
β-D-Fructofuranosyl											

^a Values are reported relative to internal HO²H (4.80 ppm) and are accurate to ±0.01 ppm.

TABLE IX

 ^1H – ^1H spin-coupling constants ^a in β -fructofuranosyl α -D-glucopyranoside (sucrose, **1**) in $^2\text{H}_2\text{O}$

Coupled nuclei	Residue	
	α -D-Glucopyranosyl	β -D-Fructofuranosyl
H-1, H-1'		–12.7
H-1, H-2	3.9	
H-2, H-3	10.0	
H-3, H-4	~ 9.5	8.8
H-4, H-5	~ 9.5	~ 8.5
H-5, H-6		~ 3.7 ^b
H-5, H-6'		~ 6.4 ^b

^a Values are reported in Hz and are accurate to ± 0.1 Hz. No entry denotes values that could not be measured. ^b Assignments may be reversed.

fragment. Endocyclic $^1J_{\text{CC}}$ are smaller than related exocyclic $^1J_{\text{CC}}$. Thus, $^1J_{\text{C-1,C-2}}$ (52.7 ± 0.3 Hz) is ~ 10 Hz larger than $^1J_{\text{C-5,C-6}}$ (42.4 ± 0.1 Hz). In both cases the C–C bond is exocyclic but the former pathway contains three oxygen substituents (O-1, O-2, O-5), while the latter contains two (O-5, O-6). Likewise, $^1J_{\text{C-2,C-3}}$ (47.1 ± 1.2 Hz) is ~ 7 Hz larger than $^1J_{\text{C-3,C-4}}$ (40.4 ± 0.9 Hz) since the former C–C bond contains an additional oxygen substituent. $^1J_{\text{C-1,C-2}}$ is ~ 6 Hz larger than $^1J_{\text{C-2,C-3}}$; both pathways include three oxygen substituents, but the former is exocyclic. Previous studies of 2-ketopentofuranoses⁹ have shown that $^1J_{\text{C-2,C-3}}$ depends on anomeric configuration, with larger values observed when O-2 and O-3 are *trans*. This relationship is maintained in 2-ketohexofuranosyl rings having the *D-fructo* configuration (**2**, 48.4 Hz; **1**, **3**, ~ 46.4 Hz).

B. Longer range spin couplings: furanose ring structure and conformation. It is well recognized that five-membered rings are conformationally flexible²⁷ and that in general nonplanar (puckered) conformers are more stable than the planar form. Two idealized nonplanar forms are possible, namely, twist (*T*) and envelope (*E*)

TABLE X

 ^{13}C – ^1H spin-coupling constants ^a in β -D-fructofuranosyl β -D-glucopyranoside (sucrose, **1**) in $^2\text{H}_2\text{O}$

Coupled nuclei	Sucrose (1)
C-1, H-3	1.7
C-2, H-1	3.2
C-2, H-1'	3.2
C-2, H-3	nc
C-2, H-4	nc
C-2, H-5	2.0
C-2, H-1 ^g	3.9
C-6, H-4	5.0

^a Values are reported in Hz and are accurate to ± 0.1 Hz. An 'nc' denotes no coupling. Atoms within the glucopyranosyl ring are denoted by a 'g' superscript; all other atoms are within the fructofuranosyl ring.

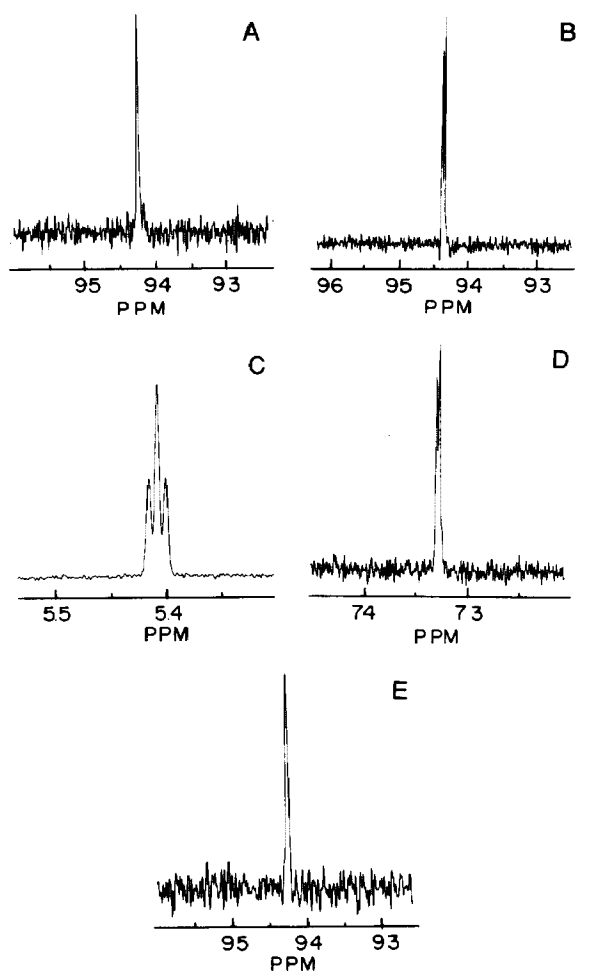


Fig. 4. Detection of ^{13}C - ^1H and ^{13}C - ^{13}C spin couplings across the *O*-glycosidic linkage of **1**. (A) The C-1^g signal of (1^f - ^{13}C)**1**. (B) The C-1^g signal of (2^f - ^{13}C)**1**. (C) The H-1^g signal of (2^f - ^{13}C)**1**. (D) The C-2^g signal of (2^f - ^{13}C)**1**. (E) The C-1^g signal of (3^f - ^{13}C)**1**. These signals yielded all of the ^{13}C - ^1H and ^{13}C - ^{13}C couplings across the glycosidic linkage of **1** (see Tables VII and X).

forms, and these may interconvert via pseudorotation or inversion^{28–30}. The former describes a circular pathway for the systematic interconversion of *T* and *E* forms that does not involve the planar form (Fig. 5). In contrast, inversion involves nonplanar interconversion via the planar form.

Since barriers to interconversion between furanose conformers are low in solution, parameters such as NMR chemical shifts and spin–spin coupling constants will be averaged in a fashion that reflects the relative populations of forms present and the dynamics of their interconversion³¹. Due to the large number of models that are possible to describe furanose conformational dynamics in solution, it is difficult to establish with confidence the correct model for a particular

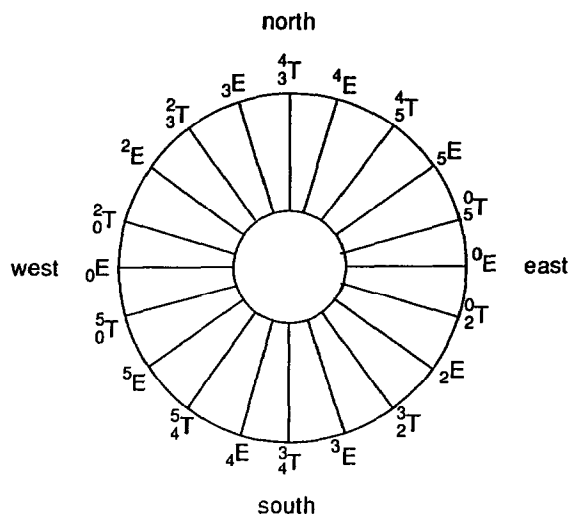


Fig. 5. The pseudorotational itinerary for a 2-ketofuranosyl ring, showing alternating envelope (*E*) and twist (*T*) forms. See text for definitions.

furanose ring from such data. The problem is particularly acute when only a few parameters are available; for example, ${}^3J_{\text{HH}}$ values are commonly used to assess furanose ring geometry, but in many cases their number is insufficient for analysis. A case in point is **2** (and **3**) where only two ${}^3J_{\text{HH}}$ values are available within the ring. Serianni and Barker³², and Cyr and Perlin³³ have suggested that J_{CH} and J_{CC} may assist the analysis in these cases, since these couplings are often abundant. In the following discussion, ${}^3J_{\text{HH}}$, ${}^3J_{\text{CH}}$, and ${}^3J_{\text{CC}}$ values are integrated in order to improve the conformational analysis of **1–3**. Furthermore, couplings in **2** and **3** are compared to corresponding couplings in α - (**4**) and β -D-threo-2-pentulofuranose (**5**) and in the β -D-fructofuranosyl component of sucrose (**1**) to assess the effects of anomeric configuration, the presence of an exocyclic hydroxymethyl group at C-5, and glycosidic bond formation (i.e., disaccharide formation) on the conformational preferences of the fructofuranosyl ring.

${}^3J_{\text{H-3,H-4}}$ and ${}^3J_{\text{H-4,H-5}}$ in **2** (3.2 Hz, 6.0 Hz) and **3** (8.2 Hz, ~ 7.5 Hz) suggest that these compounds prefer significantly different ring conformations in ${}^2\text{H}_2\text{O}$. The larger values found in **3** indicate that, on average, the H-3–H-4 and H-4–H-5 proton pairs lie in a *trans* orientation more often than they do in **2**. Thus, ${}^3J_{\text{HH}}$ data suggest a preferred “south” conformation for **2** and a preferred “north” conformation for **3** (Fig. 5). In these preferred conformations, the C-2–O-2 bond assumes a quasi- or near quasi-axial orientation, as expected from the anomeric effect³⁴. Inspection of the directly comparable ${}^3J_{\text{H-3,H-4}}$ (${}^3J_{\text{H-4,H-5}}$ cannot be directly compared due to the substituent change at C-5) between **2** (3.2 Hz) and **4** (2.9 Hz)⁹, and between **3** (8.2 Hz) and **5** (5.6 Hz)⁹, suggests that conversion from the 2-ketopentulofuranose to the 2-ketohexopentuloside causes a greater change in conformation for the β anomer than for the α anomer. Since the C-2–O-2 bond in

2 and **3** prefers a quasi- or near quasi-axial orientation, and since hydroxymethyl substituents appear to prefer quasi- or near quasi-equatorial orientations³², this result is not unexpected. In **4**, the C-2–O-2 and C-1–C-2 bonds lie in their favored orientations (quasi-axial and quasi-equatorial, respectively) in the favored conformer (near 2E)⁹. The same conformation for **2** orients the C-5–C-6 bond in its favored quasi-equatorial orientation, thus reinforcing a preferred conformation near 2E . In contrast, conversion of the preferred 2E conformer of **5** (ref 9) to the 2E conformer of **3** produces a destabilizing 1,3-interaction between O-2 and C-6, which is relieved by altering the conformational preference of the ring (i.e., a shift from 2E to 4E).

Analysis of ${}^3J_{CH}$ and ${}^3J_{CC}$ values in **2** and **3** provides support for the conformational conclusions based on ${}^3J_{HH}$. For example, ${}^3J_{C-1,H-3}$ and ${}^3J_{C-2,H-5}$ are smaller in **2** (no coupling observed) than in **3** (2.1 Hz, 2.8 Hz), whereas ${}^3J_{C-2,H-4}$ and ${}^3J_{C-2,C-6}$ are larger in **2** (1.7 Hz, 2.3 Hz) than in **3** (no coupling observed). These trends are consistent with preferred “south” conformers for **2** and preferred “north” conformers for **3**. ${}^3J_{C-3,C-6}$ is slightly smaller in **2** (2.0 Hz) than in **3** (2.5 Hz), which is also consistent with their conformational preferences.

Despite apparent preferences for south and north conformers of **2** and **3**, respectively, both compounds probably experience conformational interconversion between north and south forms to varying extents in solution, either via east (e.g., 0E) or west (e.g., 0E) forms (Fig. 5). West forms will be destabilized by 1,3-interactions involving the $-OCH_3$ or $-CH_2OH$ substituents at C-2 and the $-CH_2OH$ substituent at C-5; these interactions are absent in east forms. Thus, interconversion is likely to occur mainly via east forms.

The conversion of **3** into sucrose **1** is accompanied by an increase in ${}^3J_{H-3,H-4}$ ($\Delta = 0.6$ Hz) and ${}^3J_{H-4,H-5}$ ($\Delta = \sim 1.0$ Hz), indicating an enhanced preference for conformers having H-3–H-4 and H-4–H-5 *trans* in **1** relative to **3**. These data suggest that the β -D-fructofuranosyl ring of **1** prefers north conformations that reside in a more limited region of the pseudorotational itinerary compared to **3** and/or the potential north–south equilibrium lies more in favor of north forms for **1** than for **3**. In either scenario, the conformational mobility of the furanosyl ring in **3** appears to be reduced when incorporated into **1**. This conclusion is consistent with differences in the magnitudes of ${}^3J_{C-1,C-5}$, ${}^3J_{C-2,H-5}$, and ${}^3J_{C-3,C-6}$ between **3** and **1**. Thus, it appears that the conversion of **3** to the β -D-fructofuranosyl ring in **1** alters the conformational options of the furanosyl ring. Finally, the 2H_2O solution conformation of the fructofuranosyl ring of **1** is similar to that observed in the crystalline state (4T) (ref 1).

C. Exocyclic hydroxymethyl conformation. Two types of hydroxymethyl groups are found in **2** and **3**. The group appended to C-2 is spin isolated; the H-1 and H-1' protons generate an AB (or AM) pattern. In contrast the H-6 and H-6' protons are coupled to each other and to H-5, generating an ABX (or AMX) pattern. Three-bond 1H – 1H couplings (${}^3J_{H-5,H-6}$ and ${}^3J_{H-5,H-6'}$) are available to evaluate C-5–C-6 bond conformation. Conformation about the C-1–C-2 bond can be

assessed via $^2J_{\text{CH}}$ and $^3J_{\text{CH}}$, as discussed below.

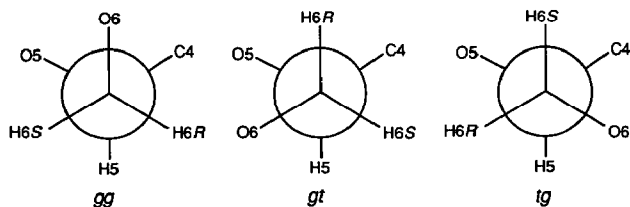


Chart 2.

The three staggered rotamers about the C-5–C-6 bond in **2** and **3** are denoted as the *gg*, *gt* and *tg* conformers (Chart 2). In the absence of stereochemical assignments of the H-6 and H-6' signals, it is not possible to determine the relative abundances of each rotamer. However, the *gg* populations can be estimated from the equation³⁵,

$$P_{gg} = \left[(J_t + J_g) - (J_{5,6} + J_{5,6'}) \right] / (J_t - J_g),$$

where J_t and J_g are standard $^3J_{\text{H,H}}$ values for the *trans* and *gauche* arrangements, and P_{gg} is the fractional population of the *gg* rotamer. If $J_t = 11.0$ Hz and $J_g = 1.5$ Hz, then P_{gg} values for **2** and **3** are 0.40 and 0.23, respectively. These values compare favorably with P_{gg} values of 0.35 and 0.20 determined previously³⁶ for the structurally related compounds, methyl α - (**6**) and β -D-arabinofuranosides (**7**) (Chart 3), respectively. Thus, P_{gg} in **2**, **3**, **6**, and **7** appears to depend, in part, on anomeric configuration, with larger values in α anomers than in β anomers. The reduced P_{gg} in **3** may be due to unfavorable interactions between O-2 (O-1 in **7**), which prefers a quasi-axial orientation, and the exocyclic CH_2OH group, whose oxygen atom orients “over” the furanose ring and is thus closer to O-2 in the *gg* rotamer.

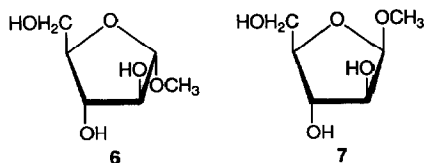


Chart 3.

The conformational behavior of the C-1–C-2 and C-2–O-2 bonds in **2** and **3** are likely to be interdependent. The exoanomeric effect^{37,38} predicts that the preferred C-2–O-2 torsion will orient the aglycone methyl carbon *gauche* to both C-1 and O-5 (*anti* to C-3). Coupling between C-3 and the aglycone methyl carbon ($^3J_{\text{C-3,OMe}}$) could, in principle, be used to assess C-2–O-2 bond conformation. $^3J_{\text{C-3,OMe}} = 2.4$ Hz and 1.8 Hz in **2** and **3**, respectively (Table III). While an appropriate Karplus curve for this C–C–O–C coupling pathway is not presently

available, these couplings are large enough to be consistent with a preferred C-2–O-2 bond torsion having C-3 and the methyl carbon *trans*. If this C-2–O-2 torsion is held constant, then three staggered rotamers about the C-1–C-2 bond are possible (Chart 4). Model inspection suggests that *gt* may be the least stable rotamer in both **2** and **3**, being destabilized by 1,3-interactions involving the aglycone methyl group. Furthermore, in the preferred ${}_2E$ conformation of **2**, the *gg* rotamer is destabilized by 1,3-interactions involving O-3, leaving the *tg* rotamer most favored. Thus, differences might be expected in the C-1–C-2 rotamer populations for **2** and **3**, since in the former two rotamers experience destabilizing interactions, whereas in the latter only one rotamer is unfavored.

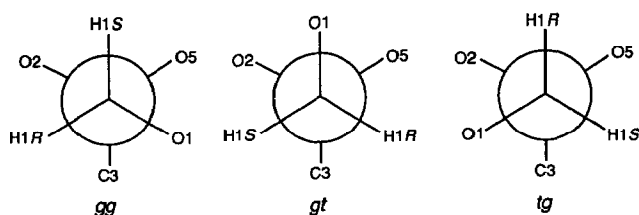


Chart 4.

^{13}C – ^1H coupling data pertinent to C-1–C-2 bond conformation in **2** and **3** are given in Table II, and those for **1** in Table X. The sum, [${}^2J_{\text{C-2,H-1}} + {}^2J_{\text{C-2,H-1}'}$], for **1**–**3** is 6.4 ± 0.1 Hz. This value is similar to that observed previously in **4** and **5** (ref 9), and suggests that the *gt* rotamer is present in least abundance. It is noteworthy that ${}^2J_{\text{C-2,H-1}} < {}^2J_{\text{C-2,H-1}'}$ in **4** and **5**, whereas ${}^2J_{\text{C-2,H-1}} > {}^2J_{\text{C-2,H-1}'}$ in **2** and **3**, suggesting that the stereochemical assignments for H-1 and H-1', or the relative populations of the *gg* and *tg* rotamers, are inverted between these compounds. Furthermore, ${}^2J_{\text{C-2,H-1}} = {}^2J_{\text{C-2,H-1}'}$ in **1**, indicating a different distribution of C-1–C-2 rotamers in **1** than exists in **3**.

In addition to ${}^2J_{\text{C-2,H-1(H-1)'}}$, ${}^3J_{\text{C-3,H-1(H-1)'}}$ (Table II) is also useful in evaluating C-1–C-2 bond conformation in **2** and **3**. The difference, [${}^3J_{\text{C-3,H-1}} - {}^3J_{\text{C-3,H-1}'}$], is greater in **2** (~ 2.2 Hz) than in **3** (0.9 Hz), which suggests a greater difference between the *gg* and *tg* populations in **2**. This result is consistent with the above rationale, since one rotamer (*tg*) appears (by inspection) highly favored in **2** whereas the *gg* and *tg* rotamer populations may be more comparable in **3**.

D. Glycosidic bond conformation. Two molecular torsion angles, phi (ϕ) and psi (ψ), define glycoside bond conformation in **1** (Chart 1). These torsion angles are defined by the H-1^g–C-1^g–O-1^g–C-2^f (ϕ) and C-1^g–O-1^g–C-2^f–O-5^f (ψ) molecular fragments. ${}^3J_{\text{C-2f,O-1g,C-1g,H-1g}}$ and ${}^3J_{\text{C-2f,O-1g,C-1g,C-2g}}$ are available to evaluate ϕ , while ${}^3J_{\text{C-1f,C-2f,O-1g,C-1g}}$, and ${}^3J_{\text{C-3f,C-2f,O-1g,C-1g}}$ may be used to assess ψ (Tables VII and X).

In the crystal structure of **1** (ref 1), $\phi = -8.0^\circ$ and $\psi = -44.8^\circ$. The observed values of ${}^3J_{\text{C-2f,H-1g}}$ (3.9 Hz) and ${}^3J_{\text{C-2f,C-2g}}$ (2.0 Hz) are consistent with the small

value of ϕ observed in the crystal structure. In the solid state, the dihedral angles for the $C-1^f-C-2^f-O-1^g-C-1^g$, $C-2^f-O-1^g-C-1^g-C-2^g$ and $C-3^f-C-2^f-O-1^g-C-1^g$ coupling pathways are $\sim 76^\circ$, $\sim 128^\circ$, and $\sim -164^\circ$, respectively (Chart 5). The observed coupling constants ($^3J_{C-1^f,C-1^g} = ^3J_{C-3^f,C-1^g} = nc$) (Table VII), however, appear to be inconsistent with the crystal value of ψ . Specifically, $^3J_{C-3^f,C-1^g}$ appears small for a $\sim 164^\circ$ angle (compare, for example, to the value of 1.8 Hz for $^3J_{C_3,CH_3}$ in **3**). A glycoside linkage geometry consistent with the data may be generated, however, by rotating the $C-2^f-O-1^g$ bond to orient $O-5^f$ and $C-1^g$ roughly antiperiplanar [thereby generating similar dihedral angles of $\sim 60^\circ$ between $C-1^f-C-1^g$ and $C-3^f-C-1^g$], and adjusting the $O-1^g-C-1^g$ torsion to generate a 140° – 150° dihedral angle between $C-2^f$ and $C-2^g$ (Chart 6). This conformation is similar to the *S*-3–*S*-4 conformations described by Tran and Brady⁸ in conformational energy calculations on **1**. These calculations indicate that *S*-3 and *S*-4 have energies ~ 2.5 kcal/mol higher than the global minimum energy structures *S*-1/*S*-2, which are closely related to the crystal structure. Thus, while the *trans*-glycoside ^{13}C - 1H and ^{13}C - ^{13}C couplings constrain the torsional options of ϕ , they do not permit the conclusion that crystal and solution (2H_2O) structures of **1** are similar with respect to ψ . The data suggest that the crystal and solution values of ϕ are likely to be similar, but of ψ may differ by $\sim 120^\circ$. In aqueous solution, the rotational excursions of ϕ may be considerably more limited than those of ψ , with the latter possibly sampling both domains in Charts 5 and 6. Of course, the above argument assumes that the small couplings observed between $C-3^f$ and $C-1^g$, and $C-1^f$ and $C-1^g$, imply similar dihedral angles, an assumption requiring validation through the construction of Karplus curves appropriate for these coupling pathways.

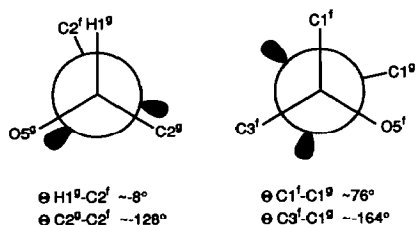


Chart 5.

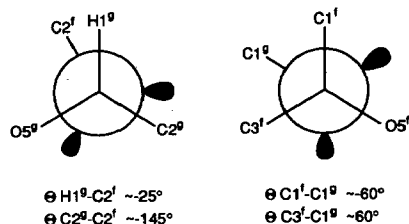


Chart 6.

The energy difference between *S*-1/*S*-2 and *S*-3/*S*-4 conformers in solution will be affected in part by the interplay between the exoanomeric effect^{37,38} and

hydrogen bonding forces. The crystal (*S*-1/*S*-2) conformation of **1** contains α -D-glucopyranosyl and β -D-fructofuranosyl rings having C-1^g-O-1^g and C-2^f-O-2^f bond torsions, respectively, (here O-1^g and O-2^f are equivalent) favored by the exoanomeric effect (i.e., C-2^f is gauche to H-1^g and O-5^g, and C-1^g is gauche to C-1^f and O-5^f). Thus, reinforcing exoanomeric factors in both residues of **1** add stability to the linkage conformation observed, and are further reinforced by intramolecular hydrogen bonding between OH-6^f \cdots O-5^g and/or OH-1^f \cdots O-2^g in the crystal. The alternate conformations (*S*-3/*S*-4) maintain the favored C-1^g-O-1^g geometry but contain an altered C-2^f-O-2^f torsion (C-1^g is gauche to C-1^f and C-3^f). While the latter geometry, considered in isolation, may be less stable than the corresponding geometry in *S*-1/*S*-2, any destabilization may be partly offset by transient intramolecular hydrogen bonding between O-1^g \cdots O-5^f, O-1^f \cdots O-5^g and/or O-3^f \cdots O-2^g, and/or a more stable hydrogen bonding structure (compared to *S*-1/*S*-2) with solvent water.

CONCLUSIONS

Site-specific ¹³C-labeling of **1** in the β -D-fructofuranosyl ring has yielded a number of ¹³C-¹H and ¹³C-¹³C spin-couplings that have been used to assess general effects of carbohydrate structure on J_{CH} and J_{CC} , and to probe the conformational preferences of **1** in solution. With respect to the former, results show that the magnitude of $^1J_{\text{CC}}$ increases with the number of electronegative substituents on the C-C fragment. This correlation, as well as potential torsional effects on $^1J_{\text{CC}}$, deserve further scrutiny, especially since $^1J_{\text{CC}}$ may be more readily measured than $^2J_{\text{CC}}$ and $^3J_{\text{CC}}$ in larger polymers. The utility of $^3J_{\text{C-1,H-3}}$ has been confirmed as a means to assess anomeric configuration of 2-ketofuranosyl rings. Editing of ¹³C NMR spectra of site-specific ¹³C-labeled carbohydrate oligomers by the INADEQUATE technique¹⁹⁻²¹ has been shown to facilitate the measurement of ¹³C-¹³C couplings in otherwise complex 1D spectra. The integration of information derived from J_{CC} , J_{CH} , and J_{HH} improves the assessment of conformationally flexible molecules or portions of molecules, such as encountered in furanosyl rings and glycosidic linkages.

The addition of substituents to a furanosyl ring does not necessarily enhance conformational heterogeneity. The effects of substitution on conformational behavior depend highly on ring configuration. For example, adding O-methyl and hydroxymethyl groups at O-1 and C-4 of α -D-threo-pentulofuranose (**4**) (to give **2**) has little effect on preferred ring conformation, whereas a considerable change is observed when β -D-threo-pentulofuranose (**5**) is similarly substituted (to give **3**). In the former case, substitution introduces new nonbonded effects that *reinforce* those already present in **4**, whereas similar substitution in **5** introduces *competing* effects that destabilize its preferred geometry.

The conformation behavior of the β -D-fructofuranosyl ring of **1** appears to differ from that of methyl β -D-fructofuranoside (**3**). In this case, disaccharide

formation alters the conformational options of the furanosyl ring. Furthermore, ^{13}C – ^1H and ^{13}C – ^{13}C spin-couplings across the glycosidic linkage suggest a ψ glycosidic torsion angle different from that observed in the crystal, whereas ϕ appears similar. The flexibility of ψ in aqueous solution may be caused in part by the dynamic interplay between exoanomeric effects^{37,38}, hydrogen bonding, and solution.

ACKNOWLEDGMENT

This work was supported by a grant from the National Institutes of Health (GM-33791) and Omicron Biochemicals, Inc. of South Bend, IN.

REFERENCES

- 1 (a) J.C. Hanson, L.C. Sieker, and J.H. Jensen, *Acta Crystallogr., Sect. B*, 29 (1973) 797–808. (b) G.M. Brown and H.A. Levy, *Acta Crystallogr., Sect. B*, 29 (1973) 790–797.
- 2 (a) M. Mathlouthi, *Carbohydr. Res.*, 91 (1981) 113–123. (b) M. Mathlouthi and D.V. Luu, *Carbohydr. Res.*, 81 (1980) 203–212.
- 3 D.B. Davies and J.C. Christofides, *Carbohydr. Res.*, 163 (1987) 269–274.
- 4 B. Mulloy, T.A. Frenkiel, and D.B. Davies, *Carbohydr. Res.*, 184 (1988) 39–46.
- 5 K. Bock and R.U. Lemieux, *Carbohydr. Res.*, 100 (1982) 63–74.
- 6 D.C. McCain and J.L. Markley, *Carbohydr. Res.*, 152 (1986) 73–80.
- 7 (a) C.H. du Penhoat, A. Imberty, N. Roques, V. Michon, J. Mentech, G. Descotes, and S. Perez, *J. Am. Chem. Soc.*, 113 (1991) 3720–3727. (b) B. Adams and L. Lerner, *J. Am. Chem. Soc.*, 114 (1992) 4827–4829.
- 8 V.H. Tran and J.W. Brady, *Biopolymers*, 29 (1990) 961–976.
- 9 T. Vuorinen and A.S. Serianni, *Carbohydr. Res.*, 209 (1990) 13–31.
- 10 A.S. Serianni, H.A. Nunez, and R. Barker, *Carbohydr. Res.*, 72 (1979) 71–78.
- 11 A.S. Serianni, T. Vuorinen, and P. Bondo, *J. Carbohydr. Chem.*, 9 (1990) 513–541.
- 12 M.L. Hayes, N.J. Pennings, A.S. Serianni, and R. Barker, *J. Am. Chem. Soc.*, 104 (1982) 6764–6769.
- 13 M.J. King-Morris, P. Bondo, R. Mrowca, and A.S. Serianni, *Carbohydr. Res.*, 175 (1988) 49–58.
- 14 S.J. Angyal, G.S. Bethell, and R. Beveridge, *Carbohydr. Res.*, 73 (1979) 9–18.
- 15 J.E. Hodge and B.T. Hofreiter, *Methods Carbohydr. Chem.*, 1 (1962) 380–394.
- 16 K. Bock and C. Pedersen, *Adv. Carbohydr. Chem. Biochem.*, 41 (1983) 27–66.
- 17 J.T. Park and M.J. Johnson, *J. Biol. Chem.*, 181 (1949) 149–151.
- 18 P.W. Austin, F.E. Hardy, J.G. Buchanan, and J. Baddiley, *J. Chem. Soc.*, (1963) 5350–5353.
- 19 A. Bax, R. Freeman, and S.P. Kempell, *J. Am. Chem. Soc.*, 102 (1980) 4849–4851.
- 20 M.J. King-Morris and A.S. Serianni, *J. Am. Chem. Soc.*, 109 (1987) 3501–3508.
- 21 J. Wu and A.S. Serianni, *Carbohydr. Res.*, 226 (1992) 209–219.
- 22 Hare Research, Inc., 14810 216th Avenue NE, Woodinville, WA 98072.
- 23 (a) B. Capon, G.W. Loveday, and W.G. Overend, *Chem. Ind. (London)*, (1962) 1537. (b) B. Capon, *Chem. Rev.*, 69 (1969) 407–498.
- 24 T. Vuorinen and A.S. Serianni, *Carbohydr. Res.*, 207 (1990) 185–210.
- 25 S.J. Angyal and G.S. Bethell, *Aust. J. Chem.*, 29 (1976) 1249–1265.
- 26 (a) H.C. Jarrell, T.F. Conway, P. Moyna, and I.C.P. Smith, *Carbohydr. Res.*, 76 (1979) 45–57. (b) K. Bock, C. Pedersen, and H. Pedersen, *Adv. Carbohydr. Chem. Biochem.*, 42 (1984) 193–213.
- 27 J. Kilpatrick, K. Pitzer and K. Spitzer, *J. Am. Chem. Soc.*, 69 (1947) 2483–2488.
- 28 C. Altona and H.J. Geise, *Tetrahedron*, 24 (1968) 13–32.
- 29 C. Altona and M. Sundaralingam, *J. Am. Chem. Soc.*, 94 (1972) 8205–8212.
- 30 C. Altona and M. Sundaralingam, *J. Am. Chem. Soc.*, 95 (1973) 2333–2344.

- 31 O. Jardetzky, *Biochem. Biophys. Acta*, 621 (1980) 227.
- 32 A.S. Serianni and R. Barker, *J. Org. Chem.*, 49 (1984) 3292–3300.
- 33 N. Cyr and A.S. Perlin, *Can. J. Chem.*, 57 (1979) 2504–2511.
- 34 R. Lemieux, in P. De Mayo (Ed.), *Molecular Rearrangements*, Wiley-Interscience, New York, 1963, p 713.
- 35 O. Jardetzky and G.C.K. Roberts, *NMR in Molecular Biology*, Academic Press, New York, 1981, p 205.
- 36 G.D. Wu, A.S. Serianni, and R. Barker, *J. Org. Chem.*, 48 (1983) 1750–1757.
- 37 R.U. Lemieux, *Pure Appl. Chem.*, 25 (1971) 527–548.
- 38 R.U. Lemieux, S. Koto, and D. Voisin, *ACS Symp. Ser.*, 87 (1979) 17.